

See discussions, stats, and author profiles for this publication at: <https://www.researchgate.net/publication/263939281>

Room-Temperature Self-Healable and Remoldable Cross-linked Polymer Based on the Dynamic Exchange of Disulfide Bonds

ARTICLE in CHEMISTRY OF MATERIALS · MARCH 2014

Impact Factor: 8.35 · DOI: 10.1021/cm4040616

CITATIONS

23

READS

137

5 AUTHORS, INCLUDING:



Hong Ping Xiang

Sun Yat-Sen University

2 PUBLICATIONS 24 CITATIONS

SEE PROFILE



Min Zhi Rong

Zhongshan University

213 PUBLICATIONS 5,742 CITATIONS

SEE PROFILE



Mingqiu Zhang

Zhongshan University

268 PUBLICATIONS 6,907 CITATIONS

SEE PROFILE

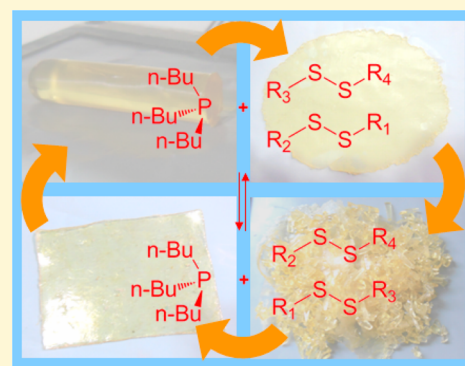
Room-Temperature Self-Healable and Remoldable Cross-linked Polymer Based on the Dynamic Exchange of Disulfide Bonds

Zhou Qiao Lei, Hong Ping Xiang, Yong Jian Yuan, Min Zhi Rong,* and Ming Qiu Zhang*

Key Laboratory for Polymeric Composite and Functional Materials of Ministry of Education, GD HPPC Lab, School of Chemistry and Chemical Engineering, Sun Yat-Sen University, Guangzhou 510275, P. R. China

Supporting Information

ABSTRACT: Tri-*n*-butylphosphine (TBP) has been shown to effectively catalyze an air-insensitive disulfide metathesis reaction under alkaline conditions at room temperature. A cross-linked polysulfide containing the phosphine exhibited repeated autonomous self-healing resulting in restoration of tensile strength as a result of the dynamic exchange of disulfide bonds. Interestingly, the cross-linked polysulfide can also be reshaped and reprocessed at room temperature via the TBP-mediated reshuffling of the macromolecular networks. The mechanical properties and self-healing ability of polymeric specimens made from chopped samples remain surprisingly constant. In sharp contrast, control specimens without the phosphine catalyst or S–S bonds are neither self-healable nor reprocessable.



INTRODUCTION

In recent years, a series of intrinsic self-healing covalent polymers based on intramolecular reversible interactions,¹ including the Diels–Alder (DA) reaction,² have been developed for structural applications. Compared with extrinsic self-healing, which occurs with the aid of microcapsules or pipelines (i.e., hollow fibers and microvascular networks),³ intrinsic self-healing does not rely on embedded healing agents and thus often allows for repeated healing. Among the available intrinsic self-healing chemistries, the disulfide bond is quite attractive because of its multiple responsive characteristics. The incorporation of this bond has enabled the self-healing of polymers under various stimuli, including heat, light, and pH.^{4–12} An additional advantage is that crack healing of polymers with disulfide bonds can take place in a one-step manner, rather than a two-step process as in the case of systems based on the DA reaction. By taking advantage of the unique properties of the disulfide bond, it should be possible to design novel, tailor-made self-healing polymers to meet the requirements of different applications.

At present, the exploration of polymeric materials that exhibit strength recovery via thermally reversible S–S bond chemistry is in its infancy. Klumperman and co-workers cured an epoxy polymer containing disulfide groups with a tetrafunctional thiol⁴ and found that the resulting material was able to fully restore its tensile failure strain at 60 °C. They attributed this recovery to the renewal of cross-links across damaged surfaces due to exchange reactions of disulfide groups. In a latter paper by the same group,⁷ the authors further investigated the healing process and concluded that the dominant mechanism is not the disulfide–disulfide exchange reaction but rather the thiol–disulfide exchange reaction. This work also determined that the

thiol groups are readily oxidized, leading to fewer possibilities for thiol–disulfide to occur.

Lafont et al. synthesized similar elastomers and demonstrated the effects of thiol cross-linkers on the cohesive and adhesive self-healing ability of these materials at 65 and 100 °C.⁶ Again, full restoration of the properties was observed. Rekondo et al. replaced the aliphatic disulfide with an aromatic disulfide to obtain a cross-linked polyurethane⁸ and found that the resulting thermoset elastomer was capable of self-healing at room temperature, as demonstrated by a healing efficiency of 97% (51% of which was due to the contribution of hydrogen bonding).

On the basis of the aforementioned pioneering works, we set out to synthesize a polymer containing disulfide bonds capable of self-healing with high healing efficiency at room temperature. Our goal was to mitigate many of the deficiencies of the existing approaches, including the thiol–disulfide exchange that is oxygen-sensitive and requires heating, and the relatively low healing efficiencies associated with aromatic disulfide exchange.

The disulfide metathesis of low-molecular-weight compounds at room temperature has been extensively studied. Caraballo et al.¹³ employed alkyl and aryl phosphines as catalysts to accelerate the disulfide metathesis of model aliphatic and aromatic disulfides at ambient temperature. Compared with triphenylphosphine, tricyclohexylphosphine exhibited better performance but poor oxidation resistance. The mechanism in this process involves the formation of a sulfur anion that attacks the disulfide bond under alkaline

Received: December 6, 2013

Revised: February 19, 2014

Published: February 20, 2014



conditions, resulting in metathesis.¹⁴ Arisawa and Yamaguchi proposed a rhodium catalyst for disulfide metathesis¹⁵ and found that the reaction proceeded rapidly in the presence of a phosphine ($\text{RhH}(\text{PPh}_3)_4$) and trifluoromethanesulfonic acid. Phosphines with electron-donating substituents (such as triarylphosphines) proved to be particularly effective.

Considering that (i) phosphines are more cost-effective than rhodium catalysts, (ii) aromatic groups are used to retard disulfide metathesis in the case of phosphines-mediated disulfide metathesis, and (iii) tricyclohexylphosphine is very sensitive to oxidation, we decided to use an aliphatic phosphine with reduced steric hindrance, tri-*n*-butylphosphine, as the catalyst in the present work to achieve our goal. Tri-*n*-butylphosphine (TBP) has previously been employed as a reducing agent to cleave disulfide bonds in aqueous media^{16–19} and has also been used to catalyze cycloaddition reactions.^{20–22} To the best of our knowledge, however, this compound has not been applied in the manner in which we used it, and we therefore investigated its performance in both low-molecular-weight and macromolecular systems.

The polymer that served as a model during our investigations was synthesized from polysulfide diglycidyl ether, using diethylenetriamine (DETA) as the hardener. We anticipated that, if the proposed disulfide metathesis proceeded, the fractured bulk cross-linked polymer would rebond with one another not only through the reconnection of cleaved S–S bonds, owing to the dynamic exchange nature of the reaction. Furthermore, such polymers might be capable of both self-healing and reprocessing by means of network reshuffling.

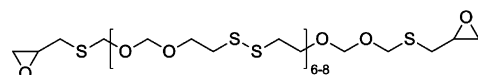
EXPERIMENTAL SECTION

Materials. Polysulfide diglycidyl ether (Thioplast EPS25, epoxide equivalent = 690 g/equiv) and polysulfide (Thioplast G44, $M_n < 1100$ g/mol; T131, $M_n = 5000$ – 7000 g/mol) were provided by AkzoNobel BV. Diethylenetriamine (DETA, 98%), 4-dimethylaminopyridine (DMAP, 98%), and 1,8-diazabicyclo[5.4.0]undec-7-ene (DBU, 98%) were purchased from Energy Chemical. TBP was obtained from the Sinopharm Chemical Reagent Co. Ltd. Poly(ethylene glycol-*block*-propylene glycol-*block*-ethylene glycol) (PEG-*b*-PPG-*b*-PEG, $M_n \approx 1100$ g/mol), dibutyl disulfide (DBDS), diethyl disulfide (DEDS), and 2,2'-hydroxy ethyldisulfide (HEDS) were purchased from Aldrich. Hydroxypropyl acrylate, tetrahydrofuran (THF, chromatographic grade), and acetonitrile (chromatographic grade) were received from Aladdin Chemical. Scheme 1 shows the structures of the substances used in this study that contained disulfide bonds.

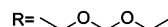
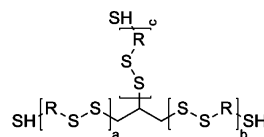
Modification of T131 and G44. A quantity of either T131 or G44 was added to hydroxypropyl acrylate to give an $n(\text{–SH})/n(\text{C}=\text{C})$ ratio of 1/1.2, after which DMAP (0.1% relative to the total mass) was added. After mixing to a uniform state under vacuum at 60 °C for 48 h to ensure complete reaction between the thiols and the double bonds, the mixture was assessed by Fourier transform infrared (FTIR) spectroscopy to identify any remaining thiol groups. In addition, the stability of the molecular chains was assessed by determining molecular weights and polydispersity index (PDI) by gel permeation chromatography (GPC). The modified T131 (M-T131) and G44 (M-G44), in which all the thiols had been consumed (Scheme 2), were subsequently used to study the disulfide exchange reaction.

Model Disulfide Metathesis Experiments. DEDS (0.31 g, 2.5 mmol), HEDS (0.39 g, 2.5 mmol), TBP (0.0021 g, 0.01 mmol), DBU (0.007 g, 0.046 mmol), and acetonitrile (10 mL) were mixed under argon by stirring at 25 °C. Samples were extracted by syringe after specific reaction times to estimate the time dependence of the disulfide metathesis. To assess the effect of the solvent, disulfide metathesis was also conducted in the absence of acetonitrile following the same procedure as above.

Scheme 1. Structures of the Disulfide Compounds

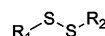


EPS25



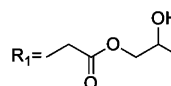
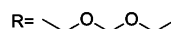
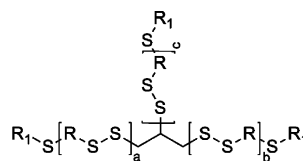
G44 ($a + b + c = n < 7$, crosslinking agent: 0.5 mol% trichloropropane)

T131 ($a + b + c = n = 30 \sim 38$, crosslinking agent: 0.5 mol% trichloropropane)



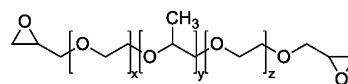
DBDS ($R_1 = R_2 = \text{C}_4\text{H}_9$), HEDS ($R_1 = R_2 = \text{C}_2\text{H}_5\text{O}$), DEDS ($R_1 = R_2 = \text{C}_2\text{H}_5$)

Scheme 2. Macromolecules Resembling the Target Polymer



M-G44 ($a + b + c = n < 7$, crosslinking agent: 0.5 mol% trichloropropane)

M-T131 ($a + b + c = n = 30 \sim 38$, crosslinking agent: 0.5 mol% trichloropropane)



PEG-*b*-PPG-*b*-PEG-EP

A typical model exchange trial involving the polysulfides was performed by mixing M-T131 (1 g), M-G44 (0.228 g), DBU (0.0122 g), TBP (0.00368 g), and THF (10 mL) with stirring under argon. Following 1 h of reaction at 60 °C, samples were extracted by syringe for the subsequent characterizations. A reaction temperature of 60 °C was applied to allow rapid screening of suitable catalysts.

Preparation of Glycidyl-End-Capped PEG-*b*-PPG-*b*-PEG. A 500 mL round-bottom three-necked flask with a mechanical stirrer was used as the reactor. Epichlorohydrin (25 g), Na hydroxide (10 g), and tetrabutylammonium hydrogen sulfate (0.2 g) were transferred into the dried reactor, which sat in an ice bath. PEG-*b*-PPG-*b*-PEG (30 g) was then added dropwise to the mixture with vigorous stirring, after which the mixture was heated to room temperature for an additional 24 h. The resulting mixture was filtered and concentrated under reduced pressure, and the crude product was dissolved in 10 mL chloroform. This solution was washed three times with 100 mL portions of pentane, and the solvent was then removed under reduced pressure, yielding glycidyl-end-capped PEG-*b*-PPG-*b*-PEG (25 g, denoted as PEG-*b*-PPG-*b*-PEG-EP, Scheme 2, epoxide equivalent = 550 g/equiv). This polymer has a similar structure to EPS25 but does not contain disulfide bonds.

Synthesis of Cross-linked Polymers. EPS25 was dried under vacuum at 80 °C for 48 h, after which equivalent amounts of EPS25 and DETA were mixed with 1 wt % DMAP and 0.3 wt % TBP and the mixture was cured. Curing was performed initially at room temperature for 3 days and then at 60 °C for 8 h to obtain the self-healing cross-linked polymer (denoted EPS-sh). To obtain a control material (denoted control-1), the same recipe and manufacturing processes were applied but without the addition of TBP. In addition, equivalent amounts of PEG-*b*-PPG-*b*-PEG-EP and DETA were mixed with 1 wt % DMAP and 0.3 wt % TBP and cured following the same procedures as were followed when making EPS-sh. The cured product was denoted control-2.

Characterization. High-performance liquid chromatography (HPLC) analyses of the model disulfides were carried out on an Agilent 1100 using a mobile phase of CH₃CN/water = 3:1 (v/v) at a flow rate of 1 mL/min with UV detection at 254 nm. Gas chromatography–mass spectroscopy (GC-MS) analyses were performed using a Thermo DSQ-EI mass spectrometer. The GC column oven was initially held at 40 °C for 1 min, followed by a ramp at 20 °C/min and a hold at 290 °C for 10 min.

GPC was performed on a Waters 1515 instrument using polystyrene as the calibration standard and THF as the eluent at a flowrate of 1 mL/min. The samples were dissolved in THF (6 mg/mL) in advance, and both the sample solutions and the THF mobile phase were filtered through 0.1 μm polytetrafluoroethylene filters. FTIR spectra of the initial monomer and the cured thermoset were recorded on a Bruker EQUINOX 55 spectrophotometer over the range of 600–4000 cm^{−1}.

Differential scanning calorimetry (DSC, TA Instrument DSC-Q10) was used to determine glass transition temperatures, *T*_g. Each sample was first cooled to −90 °C and then heated to 120 °C at a rate of 10 °C/min under a nitrogen atmosphere. Two cooling–heating cycles were run to confirm the completeness of the curing reaction.

Dynamic mechanical analysis (DMA) of film specimens (2 × 5 × 20 mm³) was performed using a Mettler Toledo Instruments DMA SDTA861 in the tensile mode under 1 Hz applying a heating ramp of 3 °C/min in nitrogen. The molecular weight between cross-links in the cured materials, *M*_c, was calculated from²³

$$M_c = 3(1 - 2/\Phi)\rho RT/E' \quad (1)$$

where *E'* is the storage modulus at the rubbery plateau zone as measured by DMA at *T* = *T*_g + 30 °C, *ρ* is the density, *R* is the gas constant, *T* is the absolute temperature, and *Φ* is the functionality of the epoxy.

All the rheological data were obtained from a strain-controlled ARG2 rheometer with 25 mm parallel-plate geometry (disk-shaped specimens: 10 mm in diameter and 2 mm in thickness). Strain sweep experiments were performed at a frequency of 1 rad/s to determine the region of linear response. Frequency sweeps from 0.01 to 300 Hz at 0.2% strain were conducted at different temperatures.

Tensile tests were performed at 25 °C on dumbbell-shaped specimens according to ISO527-2 and using a SANS CMT 6000 universal tester at a cross-head speed of 50 mm/min. To evaluate the self-healing ability of the specimens, samples were completely cut in half and then manually recombined. After rehabilitation at 25 or 60 °C for a preset period of time, these healed specimens were again subjected to tensile tests. Healing efficiency was calculated from the ratio of tensile strength of healed specimens to that of virgin specimens.

Creep behavior was measured at 25 °C according to ASTM D638-98 with a thermal mechanical analyzer (TMA, MettaviB DMA-25N) using the tensile model. Creep stress was set at 50% of the static ultimate tensile strength of each specimen.

RESULTS AND DISCUSSION

To ascertain the feasibility of using TBP as a catalyst for disulfide metathesis at room temperature, a model reaction between low-molecular-weight disulfides was initially examined. Figure 1 shows HPLC chromatograms obtained for the system

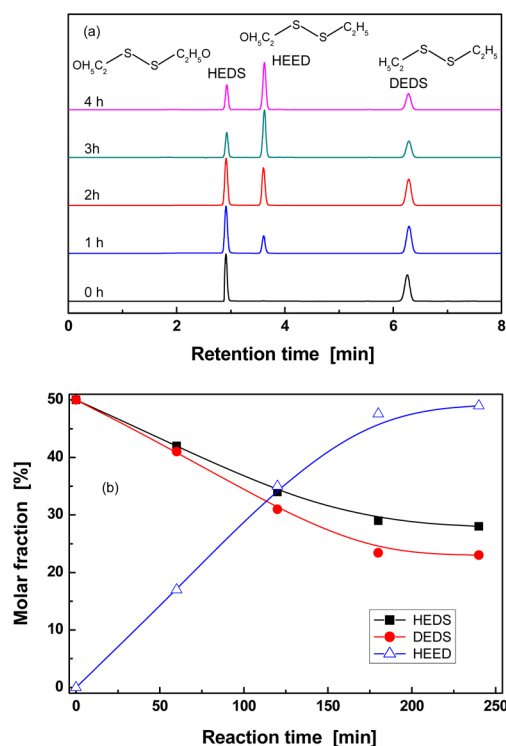


Figure 1. (a) HPLC chromatograms of mixtures containing equivalent amounts of DEDS/HEDS mixture as a function of reaction time (25 °C; 1 wt % DBU, 0.3 wt % TBP). The structure of the metathesis product HEED is evidenced by analysis of the mass spectrum (Figure S1 of the Supporting Information). (b) Molar fractions of alkyl disulfides as a function of reaction time, as determined from the data in (a).

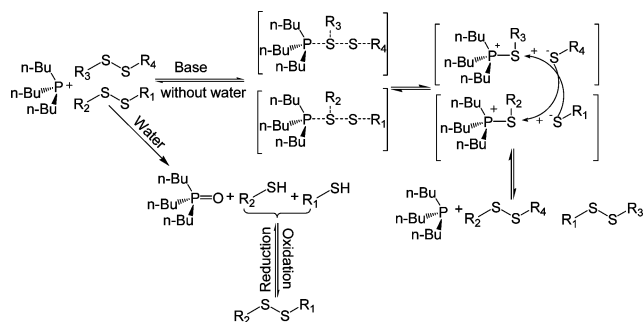
containing DEDS and HEDS in the presence of TBP and the strong base DBU. The latter was added because phosphines are known to be most effective under alkaline conditions. It is evident that, after 1 h at room temperature, the metathesis product hydroxyethyl ethyl disulfide (HEED), which is derived from DEDS and HEDS, is detected. With increasing reaction time, the molar fractions of DEDS and HEDS continuously decrease while the fraction of HEED concurrently increases. After 3 h, no further changes are seen in the relative intensities of the three peaks in the chromatogram and the proportion of HEED plateaus at ~50%. These results indicate that the exchange reaction has reached equilibrium and demonstrate that TBP can indeed catalyze room-temperature disulfide metathesis. Quantification of the reaction (Figure S2 of the Supporting Information) reveals that a linear fit to the data obtained at 25 °C gives a rate constant with regression coefficients of 0.9944 and 0.9542 for the first- and second-order plots, suggesting that the reaction likely proceeds via first-order kinetics. Similarly, the reaction at 60 °C also exhibits a higher regression coefficient for the first-order plot than for the second-order one. The activation energy derived from the first-order kinetics is 23.1 kJ/mol.

In addition, the TBP-catalyzed disulfide metathesis between DEDS and DBDS was performed in the absence of a solvent. A similar reaction equilibrium generating a 50% yield of ethyl butyl disulfide (EBDS) was determined by GC-MS analysis (Figures S3 and S4 of the Supporting Information), demonstrating that the solvent (acetonitrile in this case) has no effect on the disulfide metathesis process.

When DBU was replaced by the weak base DMAP, however, no metathesis product was obtained over the equivalent time span, even when the reaction temperature was raised to 80 °C (Figure S5 of the Supporting Information). This further highlights the dependence of the disulfide metathesis on an alkaline environment.

Caraballo et al.¹³ suggested that polar solvents may facilitate disulfide metathesis owing to the ion-pair nature of the reaction intermediate. On the basis of this theory, the metathesis reaction pathways between low-molecular-weight disulfides with catalysis by TBP are depicted in Scheme 3. Initially,

Scheme 3. TBP-Catalyzed Metathesis between Low-Molecular-Weight Disulfides



transient states are formed by reaction between the phosphine salt and the disulfides in the alkaline environment. These then dissociate into a thiolate anion and the cationic intermediate of the phosphine salt. Eventually, cross-nucleophilic attack of the thiolate anion at another sulfur atom of the cationic intermediate of the phosphine salt generates both the metathesis product and TBP. When water is present, however, the above reaction proceeds with difficulty because of the presence of phosphine oxide and thiol derivatives. For this reason, it is critical to exclude water from the reaction.

On the basis of the above model reactions, another series of model experiments was performed using polysulfides M-T131 and M-G44 as the main reactants (see Experimental Section for details). These materials contain disulfide bonds in the polymeric backbone and have much higher molecular weights than the small-molecular compounds, such that they are more similar to our target material.

As shown in Table 1, the molecular weights of M-T131/DBDS when blended with DBU and TBP are significantly lower than those of the original M-T131 or M-T131/DBDS,

while the PDI also show the same trend. These results agree with the trends in Figure 1 and suggest that disulfide metathesis can occur in polysulfides in response to catalysis by TBP. As embedding the strong base DBU in the bulk polymer could possibly induce hydrolysis of the polymeric matrix, the weak base DMAP was also examined in the above formulations. Similar reductions in molecular weight and PDI were observed when using DMAP, likely because the S–S bond energy of the polysulfides is lower than that of the low-molecular-weight disulfides.⁷ In other words, disulfide metathesis proceeds more readily in macromolecules containing disulfide bonds than in low-molecular-weight disulfides. On the basis of these results, DMAP was selected for use in conjunction with TBP in the subsequent manufacturing of self-healing cross-linked polymer from the EPS25 monomer.

In contrast, because DETA is typically used as a hardener when making cross-linked polymers, its effect on disulfide metathesis should be different. It can be seen from Table 1 that neither the molecular weight nor the PDI of M-T131/M-G44/DMAP/DETA exhibit obvious changes as compared with those of M-T131/M-G44. This situation is analogous to that of M-T131/DBDS in the absence of any other chemicals. Nevertheless, the molecular weights and PDIs of both M-T131/M-G44/DETA/TBP and M-T131/DBDS/DETA/TBP are changed following the reaction. Clearly, therefore, DETA can also function as a weak base and thus enhance the catalytic effect of the TBP. Despite this effect, because DETA is consumed when the cross-linked polysulfide is cured, it is present in the cured material at only very low levels and thus the addition of DMAP is still necessary.

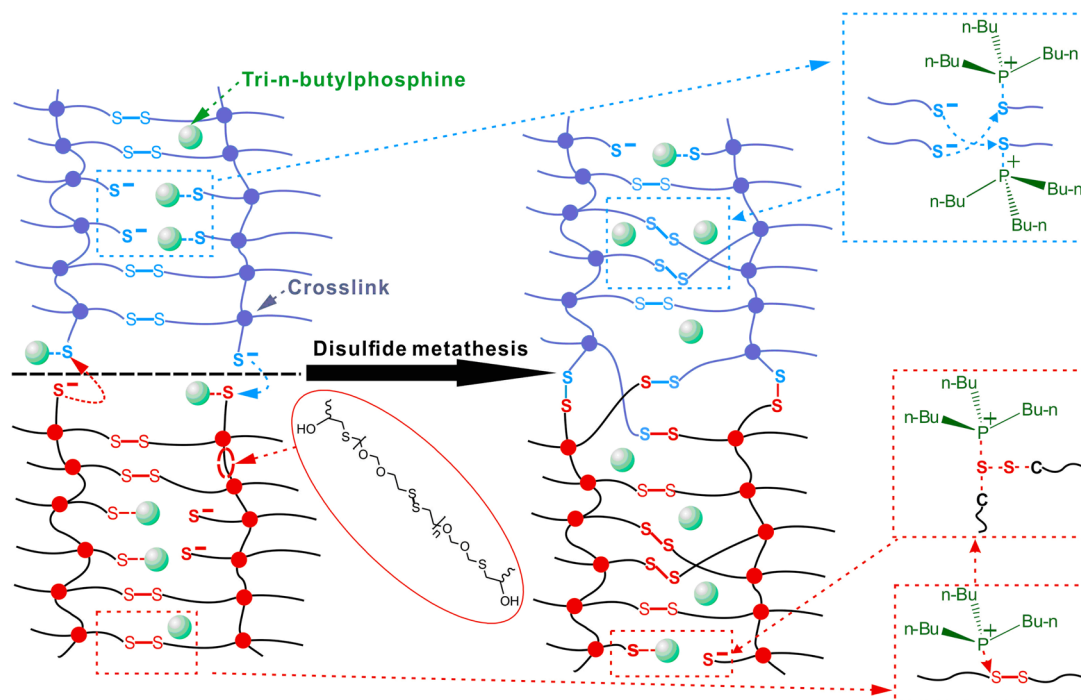
Because the model experiments have confirmed that disulfide metathesis will take place in macromolecules with the aid of TBP and DMAP, we proceeded to cure EPS25 with DETA in the presence of TBP and DMAP, producing the cross-linked polymer EPS-sh. Scheme 4 shows the envisaged disulfide metathesis of the polysulfide network as catalyzed by TBP. On the basis of the action of the organophosphorus compound, transient states are formed between the phosphine salts and the disulfide bonds in the polymer. Subsequently ion-pair intermediates consisting of thiolate anions and phosphine salt cations are generated on the macromolecular chains. As a result of the movement of chain segments at room temperature, cross nucleophilic attack of thiolate anions to other sulfur atoms by phosphine salt cationic intermediates occurs, leading to exchanges of networked chains. Meanwhile, the catalyst returns to its original state. Because this disulfide metathesis in the

Table 1. Disulfide Exchanges of Linear Polymers Containing Disulfide Bonds

materials	DBU	DMAP	DETA	TBP	$M_n (\times 10^3)$	$M_w (\times 10^3)$	PDI
M-T131	0	0	0	0	8.0	17.4	2.2
M-G44	0	0	0	0	1.7	2.5	1.5
M-T131/M-G44 ^a	0	0	0	0	4.0	12.6	3.2
M-T131/DBDS ^a	0	0	0	0	9.4	14.9	1.9
M-T131/DBDS	1 wt %	0	0	0.3 wt %	5.0	6.2	1.3
M-T131/DBDS	0	1 wt %	0	0.3 wt %	5.2	6.4	1.2
M-T131/DBDS	0	0	1 wt %	0.3 wt %	3.7	8.7	2.4
M-T131/M-G44	1 wt %	0	0	0.3 wt %	2.8	6.2	2.2
M-T131/M-G44	0	1 wt %	0	0.3 wt %	2.8	6.6	2.3
M-T131/M-G44	0	1 wt %	1 wt %	0	3.8	11.8	3.1
M-T131/M-G44	0	0	1 wt %	0.3 wt %	3.7	9.4	2.5

^aBoth M-T131/M-G44 and M-T131/DBDS are equimolar.

Scheme 4. TBP-Catalyzed Disulfide Metathesis within a Polysulfide Network



polymer networks repeats itself, rearrangement of the network structure and constant reshuffling of the molecular chains should take place. As a result, the cross-linked polymer should exhibit not only self-healing but also reprocessability based on the dynamic exchanges of disulfide bonds in the presence of the phosphine salt catalyst.

Prior to any discussion of the self-healing performance of the polysulfides, it was vital to obtain some fundamental structural information concerning the polymers. Infrared spectroscopy was used to examine the effect of curing with DETA on the oxirane rings of EPS25. Figure 2a shows that the stretching band of the oxirane rings of EPS25 (at $820\text{--}850\text{ cm}^{-1}$) disappears in the spectra of EPS-sh and control-1, indicating that the system is fully cured. This conclusion is also supported by the data resulting from DSC and DMA tests. As shown in Figure 2b, no exothermic events are observed on repeated DSC scans while the T_g of EPS-sh remains unchanged. Figure 2c also reveals that only one $\tan \delta$ peak appears, and its position, a measure of T_g , does not change during multiple measurements.

On the basis of the DMA results and using eq 1, the molecular weight between the cross-links of EPS-sh, M_c , is estimated to be 4.1×10^3 , which is much higher than that of control-1 (1.6×10^3). This implies that the degree of cross-linking of the former is lower than that of the latter. This occurs because disulfide metathesis in EPS-sh leads to a dynamic equilibrium between random disconnections and reconnections of S–S bonds. During the DMA tests, a certain fraction of S–S bonds are ruptured, and consequently the relative molecular weight between cross-links of EPS-sh appears to be higher than that of control-1 in which disulfide metathesis does not occur because of the absence of TBP. This analysis is evidenced by the higher T_g but lower $\tan \delta$ peak height of control-1 (Figure S6 of the Supporting Information), as the macromolecules are less mobile because of the restraint induced by the higher cross-linking density. In addition, the $\tan \delta$ peak of control-1 is roughly symmetrical, while that of EPS-sh has a shoulder on the

higher temperature side, which may originate from dissociation/recombination of S–S bonds.

Nevertheless, EPS-sh chains are still sufficiently cross-linked. Following immersion in the good solvent THF for 7 days at room temperature, for example, the material is not dissolved but still maintains its structural integrity, exhibiting only volume expansion (Figure S7 of the Supporting Information).

To gain further insight into the dynamic exchange behavior of disulfide bonds in the polymer EPS-sh, rheological measurements as a function of angular frequency were conducted (Figure 3). Figure 3a shows that the storage shear modulus, G' , decreases with decreasing frequency, while the loss shear modulus, G'' , initially decreases with decreasing frequency and then increases. The two curves intersect at a specific frequency, meaning that the rheological behavior of the specimen is no longer dominated by elastic-like behavior ($G' > G''$) but by viscous-like behavior ($G' < G''$) at low frequency. Disulfide metathesis can account for this variation; at certain low frequencies (for a given temperature), the disulfide exchange will begin to have a greater effect on rheological performance because the disconnected network needs time to be reconstructed during metathesis.

A careful examination of the curves in Figure 3a shows that the crossover frequency between G' and G'' increases with increasing temperature. Because this frequency is related to the dissociation rate constant of the reversible network,²⁴ the results of Figure 3a imply that the disulfide exchange is accelerated with a rise in temperature. This is understandable and is in agreement with the general behavior of reversible reactions. Owing to the restricted frequency range of the rheometer, however, measurements were not made at frequencies lower than 10^{-2} Hz and therefore do not show that the exchange reaction is not allowed at lower temperatures.

For reference purposes, the rheological behaviors of materials control-1 and control-2 are given in parts b and c of Figure 3, respectively. It is interesting to see that the G' and G'' curves

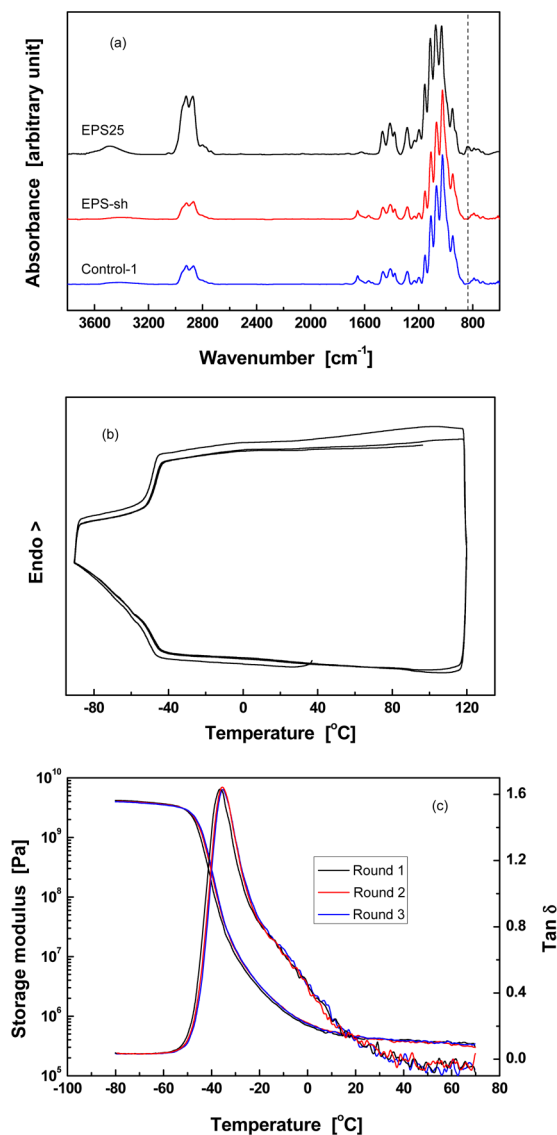


Figure 2. (a) FTIR spectra of EPS-sh and control-1 compared with that of EPS25. (b) Repeated DSC heating-cooling scans of EPS-sh. (c) Storage modulus and $\tan \delta$ of EPS-sh as a function of temperature as obtained by repeated DMA scans.

intersect at 100 °C (Figure 3b), meaning that disulfide metathesis might be enabled even without TBP catalysis. As seen in the comparison of parts a and b of Figure 3, the crossover frequency of EPS-sh at 100 °C is obviously higher than that of control-1, which illustrates once again the important role of TBP. In the case of control-2, which does not contain any S–S bonds, the material behaves like other polymers with permanent covalent bonds. Its G' is independent of frequency ($G' > G''$) over the entire frequency range.

Disulfide metathesis has been found to be possible in EPS-sh and thus should enable self-healing of the cross-linked polysulfide (Scheme 4). Figure 4a shows that this is indeed the case; the cut EPS-sh regains its tensile strength after the two fracture surfaces are brought together. The healing efficiency increases with increasing time; after 8 h, about 50% of the original strength is restored. Equilibrium state maximum healing (91%) is observed after 24 h, indicating almost full recovery. Further extending the healing time to 48 h does not lead to any increased strength in the healed specimen. To our

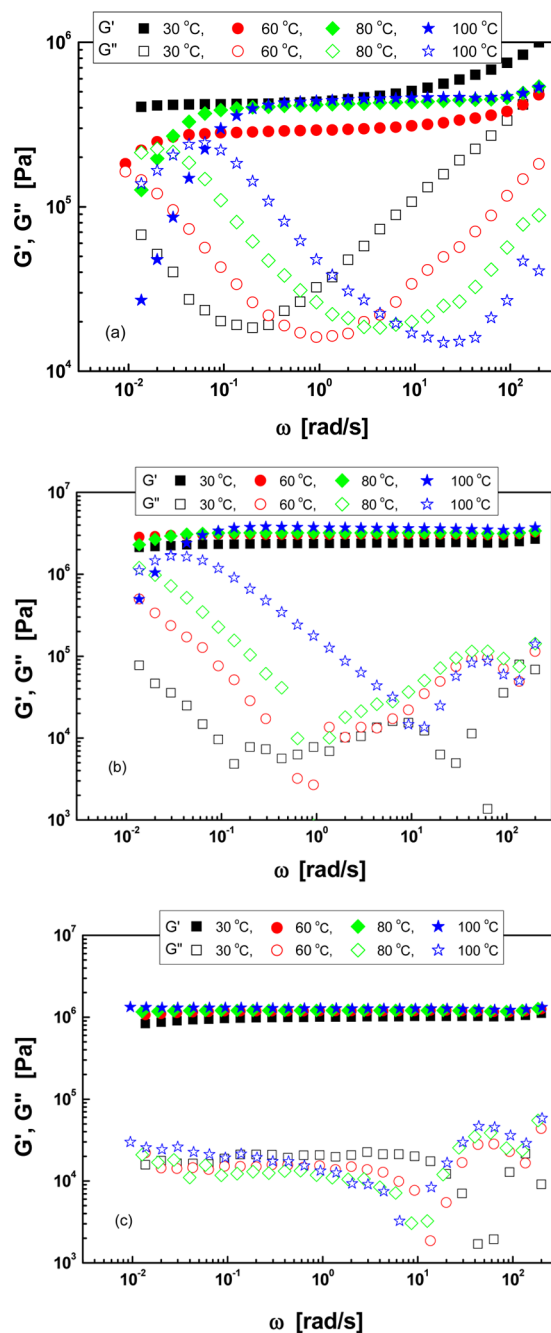


Figure 3. Storage shear modulus, G' , and loss shear modulus, G'' , as functions of oscillatory frequency, ω , for (a) EPS-sh, (b) control-1, and (c) control-2.

knowledge, a room-temperature healing efficiency of ~91% can be considered as quite a remarkable result for an intrinsic self-healing thermoset material.

Figure 4b indicates that EPS-sh can be repeatedly healed. Because the tensile strength of the virgin specimen cannot be completely restored, the reconnected interface becomes the weakest part and thus tends to break again during the subsequent tensile tests. This ensures that the second and third tensile failures occur at the same healed portion. The slight decline of efficiency of the second and third healings can be explained by misalignment of the fractured surfaces. This multiple healing ability is exclusive for intrinsic self-healing

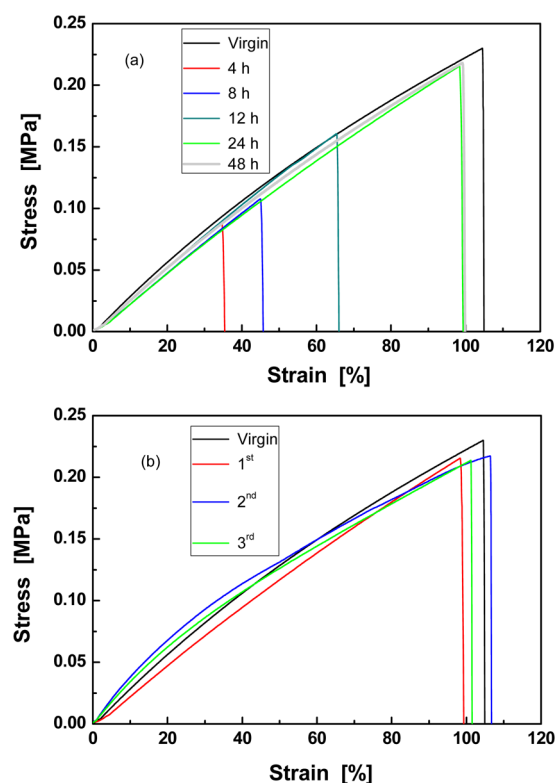


Figure 4. Typical tensile stress–strain curves of virgin and healed EPS-sh: (a) effect of healing time and (b) effect of repeated repair (healing time = 24 h). Healing temperature = 25 °C.

materials and represents a valuable feature that distinguishes these materials from extrinsic self-healing versions.

When the healing temperature was raised to 60 °C, a similar healing effect was observed, although only 2 h was sufficient to achieve equilibrium healing (Figure S8 of the Supporting Information). This finding is in good agreement with the results of the above rheology study; that is, disulfide exchange becomes faster at higher temperatures.

Tensile tests of the control materials were also performed. In the case of control-1, a marginal healing efficiency of ~13% was observed during the first healing (Figure S9 of the Supporting Information), which is primarily attributed to both dangling chains²⁵ and hydrogen bonding. The dangling chains represent strands of the fractured networks of the cross-linked polymer that are attached to the undamaged network at one end. These strands have relatively high mobility and help to establish hydrogen bonding among the interdiffused macromolecules across the intimately contacted fractured surfaces. In the case of control-2, which does not contain disulfide bonds, essentially no healing effect was detected. From the above discussions, we know that the disulfide metathesis reaction plays the primary role in the self-healing process.

The effect of exposure of the broken specimens to air was also investigated by intentionally separating the two halves of cut specimens for a time before recombination for healing. Tensile tests showed that high healing efficiency was still obtained even after an isolation time of 72 h (Figure S10 of the Supporting Information). This behavior differs from that of intrinsic self-healing polymers, which function via H-bonding, because these materials tend to lose their healing ability after long-term separation of the broken surfaces due to self-combination of neighboring free hydrogen bonds.²⁶ In contrast,

metathesis of the disulfide bonds is always in dynamic equilibrium; thus, the number of disulfide bonds available for healing does not decrease whether or not the cut surfaces are in contact with each other.

The air-insensitivity of EPS-sh was also established by another group of tests (Figure S11 of the Supporting Information) in which samples were evaluated 1 month after manufacture and were found to repeatedly self-heal to the same extent as the fresh samples (Figure 4). Theoretically, TBP may be converted into phosphine oxide and thiol derivatives as a side-reaction of disulfide metathesis when water and oxygen are simultaneously present.¹⁴ Because EPS-sh is hydrophobic, however, this side reaction tends not to proceed inside the polymer. Even though the surfaces of the polymer are in contact with the moisture in ambient air, the butyl groups of the TBP would tend to shield the phosphorus atoms from any negative effects. Consequently, the polymer is not sensitive to air exposure.

Classical thermoset materials contain permanent covalent cross-links and thus cannot be reprocessed and reshaped in the same manner as thermoplastics. In such cases, decomposition of the polymer takes place before the flowing temperature is reached. Since the development of covalent adaptable networks,²⁷ however, the idea of introducing dynamic connections that are able to undergo reversible exchange to form cross-linked materials and thus impart thermal reprocessability to these materials has been reported by several research groups.^{28–33} When considering the disulfide metathesis system developed in this work, we anticipated that the cross-linked epoxidized polysulfide should be capable of remolding without heating. To date, there are no literature reports of thermosets that exhibit room-temperature reprocessability in this manner.

Parts a and b of Figure 5 show that a cylinder-shaped specimen of EPS-sh could indeed be reshaped into a sheet morphology after compression at room temperature for 24 h. The disulfide metathesis, therefore, must have resulted in rearrangement of the cross-linked networks inside the speci-

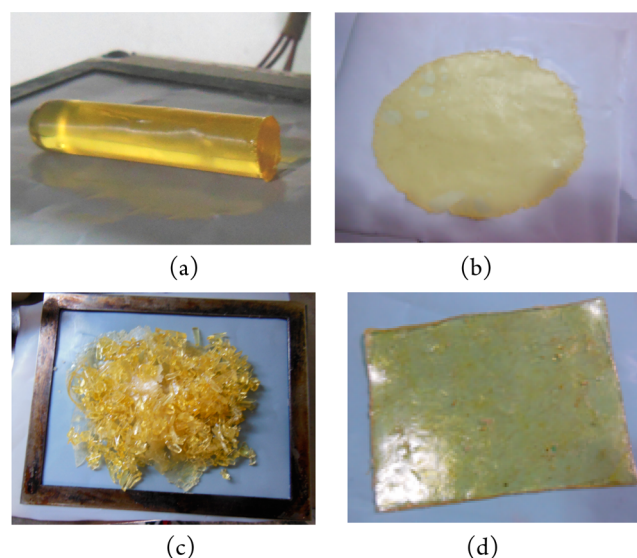


Figure 5. (a and b) Reshaping and (c and d) reprocessing of EPS-sh through compression molding at 25 °C for 24 h. Pressure = 4.5 MPa. The chopped EPS-sh shown in (c) was exposed to air for 48 h at 25 °C before remolding, and the results thus demonstrate the air-insensitivity of the polymer.

men. To further verify the recyclability of the material, the round sheet specimen of EPS-sh was cut into small pieces (Figure 5c) and then remolded into a square shape (Figure 5d) at room temperature. In comparison, the control-1 and control-2 materials could not be reprocessed under the same conditions (Figure S12 of the Supporting Information) because of a lack of disulfide metathesis in these substances.

Unlike some reversible reaction-assisted intrinsic self-healing polymers (polyurethane carrying alkoxyamine,³⁴ for example), in which re-establishment of intramolecular interactions only takes place among disconnected bonds, reconstruction of a new cross-linked network in terms of disulfide metathesis does not necessarily take place at the sites of ruptured S–S bonds (Scheme 4). The reaction depends on intermediates-induced rearrangement of networked chains and proceeds so long as the polymers are in close contact with each other. By making use of this feature, reprocessing of the cross-linked polymer is possible. In other words, not every reversible reaction that is capable of giving a self-healing polymer will lead to reprocessability, while reprocessability might serve as a criterion for metathesis. Because disulfide metathesis is responsible for the self-healing and reprocessing effects, the molded surfaces of EPS-sh specimens are not sticky to the touch, which will be a useful feature with regard to handling during practical applications.

In principle, the recycled cross-linked polymer should also be self-healable through disulfide metathesis, just as was the original specimen. As shown in Figure 6, the virgin recycled

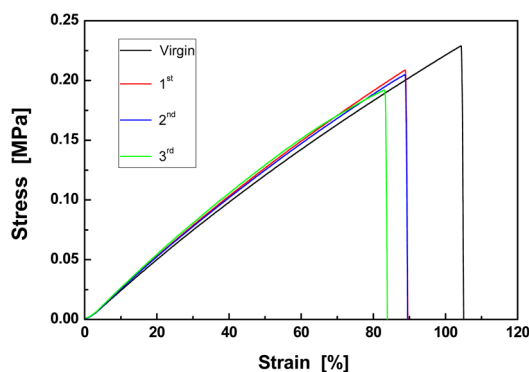


Figure 6. Typical tensile stress–strain curves of recycled EPS-sh subjected to successive breakage and healing events. Healing temperature = 25 °C; healing time = 24 h.

specimen had a tensile strength of 0.23 MPa and failure strain of 104%, both of which are equal to the values measured prior to recycling of the specimen (Figure 4). After 24 h of healing at 25 °C, the tensile strength of the recycled specimen after its first repair was 0.21 MPa, equaling ~91% of the initial value. The subsequent healing data demonstrate that the multiple self-healing ability of EPS-sh is not affected by reprocessing.

To gain a better understanding of this self-healing polymer, creep tests were carried out at room temperature (Figure 7). In general, a creep strain versus time curve obtained with plastics materials consists of four stages:³⁵ (i) initial rapid elongation, which is independent of time and arises from the elastic and plastic deformations of the polymer; (ii) primary creep, during which the creep rate starts at a relatively high value and then decreases with time; (iii) secondary creep; and (iv) tertiary creep, in which the creep rate increases rapidly and eventually results in creep fracture. Here the virgin self-healing specimen

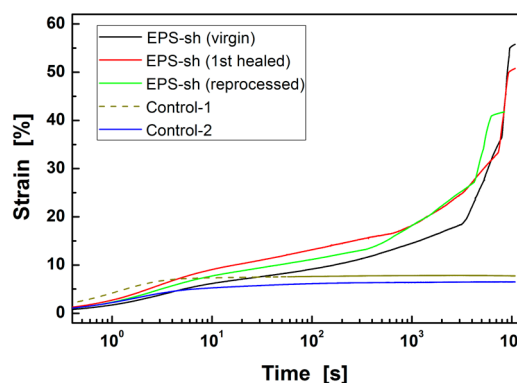


Figure 7. Typical tensile creep strain–time curves for EPS-sh and the control specimens, measured at 25 °C.

EPS-sh exhibited an insignificant initial rapid elongation stage within the creep curve. Subsequently, the above-noted primary creep was observed, while the transition to the secondary creep was somewhat inconspicuous. The tertiary creep stage lasted for a particularly long time. Both the healed and reprocessed EPS-sh had similar creep behaviors. In contrast, the two control specimens only showed the first three stages of creep within the time span tested, and no tertiary creep was observed. Moreover, their strains due to secondary creep were nearly independent of time and were lower than those of the self-healing specimens.

Although the detailed deformation mechanisms involved require further investigation, the differing molecular structures of these materials are likely responsible for the varying creep properties. The self-healing specimen EPS-sh is capable of disulfide metathesis at room temperature, and thus rearrangement of the network structure as a result of bond exchange would certainly result in creep or stress relaxation.⁷ As for the control materials, because they lack the capability for network rearrangement, their cold flow is restricted to a much greater extent under the same conditions, so that both creep rate and strain are lower than those of EPS-sh. The reduced creep resistance of EPS-sh is a deficit of the material with regard to eventual practical applications, and products made from this type of polymer would have to avoid working under persistent relatively high stress.

CONCLUSIONS

Tri-*n*-butylphosphine has proven to be an effective catalyst for promoting air-insensitive metathesis in disulfide-containing polymers. By taking advantage of this reaction, cross-linked epoxidized polysulfides can be self-healed at room temperature without manual intervention as evidenced by repeated restoration of tensile strength. Moreover, these polymers can also be reshaped and reprocessed via room-temperature compression through rearrangements of the cross-linked network in terms of the dynamic exchange of disulfide bonds. The reprocessed polymers possess mechanical properties and self-healing ability similar to those of the original materials. The de-cross-linking that is typically involved in reclaiming thermosets was found to be unnecessary during room-temperature reprocessing of these new materials. The strategy developed in this work could lead to a new means of synthesizing for recyclable cross-linked polymers and thus could mitigate fossil oil consumption to some extent.

■ ASSOCIATED CONTENT

■ Supporting Information

Figure S1, mass spectrum; Figure S2, reaction kinetics; Figure S3, gas chromatogram; Figure S4, mass spectrum; Figure S5, HPLC analyses; Figure S6, DMA curves; Figure S7, swelling test; Figures S8–S11, tensile stress–strain curves; Figure S12, reprocessing of control specimens (PDF). This material is available free of charge via the Internet at <http://pubs.acs.org>.

■ AUTHOR INFORMATION

Corresponding Author

*M. Z. Rong: cesrmz@mail.sysu.edu.cn. M. Q. Zhang: ceszmq@mail.sysu.edu.cn.

Notes

The authors declare no competing financial interest.

■ ACKNOWLEDGMENTS

The authors wish to thank the Natural Science Foundation of China (Grants 51273214, 20874117, 51073176 and 51333008), the Doctoral Fund of the Ministry of Education of China (Grant 20090171110026), the Science and Technology Program of Guangdong Province (Grants 2010B010800021, 2010A011300004, 2011A091102001, and S2013020013029), and the Basic Scientific Research Foundation in Colleges and Universities of Ministry of Education of China (Grant 12lgjc08) for financial support.

■ REFERENCES

- (1) Zhang, M. Q.; Rong, M. Z. *Polym. Chem.* **2013**, *4*, 4878.
- (2) Liu, Y.-L.; Chuo, T.-W. *Polym. Chem.* **2013**, *4*, 2194.
- (3) Zhang, M. Q.; Rong, M. Z. *Self-healing Polymers and Polymer Composites*; John Wiley & Sons, Inc.: Hoboken, NJ, 2011.
- (4) Canadell, J.; Goossens, H.; Klumperman, B. *Macromolecules* **2011**, *44*, 2536.
- (5) Yoon, J. A.; Kamada, J.; Koynov, K.; Mohin, J.; Nicolay, R.; Zhang, Y. Z.; Balazs, A. C.; Kowalewski, T.; Matyjaszewski, K. *Macromolecules* **2012**, *45*, 142.
- (6) Lafont, U.; van Zeijl, H.; van der Zwaag, S. *ACS Appl. Mater. Interfaces* **2012**, *4*, 6280.
- (7) Pepels, M.; Pilot, I.; Klumperman, B.; Goossens, H. *Polym. Chem.* **2013**, *4*, 4955.
- (8) Rekondo, A.; Martin, R.; Ruiz de Luzuriaga, A.; Cabanero, G.; Grande, H. J.; Odriozola, I. *Mater. Horiz.* **2014**, *1*, 237.
- (9) Fairbanks, B. D.; Singh, S. P.; Bowman, C. N.; Anseth, K. S. *Macromolecules* **2011**, *44*, 2444.
- (10) Amamoto, Y.; Otsuka, H.; Takahara, A.; Matyjaszewski, K. *Adv. Mater.* **2012**, *24*, 3975.
- (11) Michal, B. T.; Jaye, C. A.; Spencer, E. J.; Rowan, S. J. *ACS Macro Lett.* **2013**, *2*, 694.
- (12) Deng, G. H.; Li, F. Y.; Yu, H. X.; Liu, F. Y.; Liu, C. Y.; Sun, W. X.; Jiang, H. F.; Chen, Y. M. *ACS Macro Lett.* **2012**, *1*, 275.
- (13) Caraballo, R.; Rahm, M.; Vongvilai, P.; Brinck, T.; Ramstrom, O. *Chem. Commun.* **2008**, *48*, 6603.
- (14) Caraballo, R. Ph.D. Thesis, Royal Institute of Technology, Stockholm, Sweden, 2010.
- (15) Arisawa, M.; Yamaguchi, M. *J. Am. Chem. Soc.* **2003**, *125*, 6624.
- (16) Humphrey, R. E.; Potter, J. L. *Anal. Chem.* **1965**, *37*, 164.
- (17) Bapat, A. P.; Ray, J. G.; Savin, D. A.; Sumerlin, B. S. *Macromolecules* **2013**, *46*, 2188.
- (18) Tesoro, G. C.; Sastri, V. J. *J. Appl. Polym. Sci.* **1990**, *39*, 1425.
- (19) Sastri, V. R.; Tesoro, G. C. *J. Appl. Polym. Sci.* **1990**, *39*, 1439.
- (20) Li, E.; Jia, P.; Liang, L.; Huang, Y. *ACS Catal.* **2014**, *4*, 600.
- (21) Denmark, S. E.; Beutner, G. L. *Angew. Chem., Int. Ed.* **2008**, *47*, 1560.
- (22) Fan, R.-H.; Hou, X.-L. *J. Org. Chem.* **2003**, *68*, 726.

- (23) He, M. J.; Chen, W. X.; Dong, X. X. *Polymer Physics*, 2nd ed.; Fudan University Press: Shanghai, 2000.
- (24) Roberts, M. C.; Hanson, M. C.; Massey, A. P.; Karren, E. A.; Kiser, P. F. *Adv. Mater.* **2007**, *19*, 2503.
- (25) Yamaguchi, M.; Ono, S.; Terano, M. *Mater. Lett.* **2007**, *61*, 1396.
- (26) Cordier, P.; Tournilhac, F.; Soulie-Ziakovic, C.; Leibler, L. *Nature* **2008**, *451*, 977.
- (27) Kloxin, C. J.; Scott, T. F.; Adzima, B. J.; Bowman, C. N. *Macromolecules* **2010**, *43*, 2643.
- (28) Watanabe, M.; Yoshie, N. *Polymer* **2006**, *47*, 4946.
- (29) Zhang, Y.; Broekhuis, A. A.; Picchioni, F. *Macromolecules* **2009**, *42*, 1906.
- (30) Kloxin, C. J.; Scott, T. F.; Adzima, B. J.; Bowman, C. N. *Macromolecules* **2010**, *43*, 2643.
- (31) Montarnal, D.; Capelot, M.; Tournilhac, F.; Leibler, L. *Science* **2011**, *334*, 965.
- (32) Zheng, P.; McCarthy, T. J. *J. Am. Chem. Soc.* **2012**, *134*, 2024.
- (33) Zhang, J.; Niu, Y.; Huang, C.; Xiao, L.; Chen, Z.; Yang, K.; Wang, Y. *Polym. Chem.* **2012**, *3*, 1390.
- (34) Zhang, Z. P.; Rong, M. Z.; Zhang, M. Q.; Yuan, C. *Polym. Chem.* **2013**, *4*, 4648.
- (35) Shi, X. B.; Wu, C. L.; Rong, M. Z.; Czigany, T.; Ruan, W. H.; Zhang, M. Q. *Chin. J. Polym. Sci.* **2013**, *31*, 377.